Z. Wang, T. Zhang, X. Wu, X Huang (2022) *Predicting Transient Building Fire Based on External Smoke Images and Deep Learning*, **Journal of Building Engineering**, 47, 103823. https://doi.org/10.1016/j.jobe.2021.103823

Predicting Transient Building Fire Based on External Smoke Images and Deep Learning

Zilong Wang[1,2], Tianhang Zhang[1], Xiqiang Wu[1,*], Xinyan Huang[1,*]

[1]*Research Centre for Fire Safety Engineering, Department of Building Environment and Energy Engineering, The Hong Kong Polytechnic University, Kowloon, Hong Kong*

[2]*Research Institute for Sustainable Urban Development, Hong Kong Polytechnic University, Hong Kong*

**Corresponding to xiqiang.wu@polyu.edu.hk (X. Wu), xy.huang@polyu.edu.hk (X. Huang)*

Abstract:

A real-time evaluation of fire severity inside a building could facilitate decision-making in firefighting and rescue operations. This work explores the real-time prediction of transient fire scenarios by using external smoke images and deep learning algorithms. A big database of 1,845 simulated compartment fire scenarios is formed. Three input parameters (constant fire heat release rate, opening size, and fuel type) are paired with the external smoke images, and then trained by Convolutional Neural Network (CNN) model. Results show that by training either the front-view or side-view smoke images, the AI method can well identify the transient fire heat release rate inside the building, even without knowing the burning fuels, and the error is no more than 20%. This work demonstrates that the deep learning algorithms can be trained with simulated smoke images to determine the hidden fire information in real-time and shows great potential in smart firefighting applications.

Keywords: *Artificial intelligence; Smart firefighting; Compartment fire model; Fire recognition*

Nomenclature

Symbols		*FDS*	Fire dynamics simulator
A	area of the opening (m^2)	*FFT*	Fast Fourier Transform
H	height of the opening (m)	*HRR*	Heat release rate
Abbreviation		*LES*	Large Eddy Simulation
AI	Artificial intelligence	*MSE*	Mean squared error
ANN	Artificial neural network	*ReLU*	Rectified linear units
CFD	Computational fluid dynamics	*SYR*	Soot yield rate
CNN	Convolution neural network	*VGG*	Visual Geometry Group

1. Introduction

For a building fire, the heat release rate (HRR) is one of the most critical parameters in characterizing the fire behavior and hazard [1]. Inside a room or compartment, the fire HRR is a key parameter for judging critical events, such as the flashover and burning duration [2,3], conducting fire suppression operations, and making fire rescue decisions [4]. Although the state-of-the-art numerical models can predict fire development and smoke motion, these models rely on the temperature data from sensor networks that are not available in most buildings [5–9]. For firefighting and rescuing in a real building fire, firemen can only judge or guess the fire scenario inside based on experiences and external information, such as the smoke plume size and color. The lack of accurate fire information inside the building can lead to misjudgment of fire scenarios and critical events, e.g., flashover and backdraft, the delay in firefighting and rescue, and many injuries and fatalities. Therefore, an accurate and real-time fire prediction system, based on external fire information, is needed to protect firefighters and support decision-making.

So far, many efforts have been made to determine the internal fire HRR inside the building. The most direct way to measure the HRR is a full-scale room oxygen calorimeter, but this method can only be used in the controlled lab environment [10–12]. To achieve an effective and fast determination of fire HRR, the installation of sensor networks inside the building and applying the data-driven methods became a new approach [5–9]. By using the sensor data as the input, the compartment fire can be predicted and corrected through numerical models. The optimization methods are also used to compare modeled data with the real sensor data to help determine the fire HRR. Different optimization algorithms have been used in fire detection and prediction, such as exhaustive search [13,14], genetic algorithm [15], and gradient-based algorithms [16–19]. Nevertheless, these in-situ computational approaches can hardly predict the transient fire in real-time due to the long computation time.

More recently, artificial intelligence (AI) methods, particularly machine learning, have been applied to reveal hidden fire information and forecast fire development. For example, Kim and Lattimer [20] established a classification model to identify fire and smoke in real-time to support autonomous navigation for smart firefighting robots. Wu et al. [21–23] applied the deep learning method to forecast the tunnel fire development and smoke transportation 60 s in advance and demonstrated the smart firefighting system in a laboratory-scale tunnel model. Innovative AI tools have also been developed to assist the fire engineering performance-based design for complex buildings [24,25]. For compartment fires, Dexters et al. [26] adopted a machine learning method to determine the occurrence of flashover under given fire scenarios. Wang et al. [27] proposed a data recovery algorithm, ‘P-flash’, which can recover the missing data in case of a sensor was destroyed in a multi-room fire. Zhang et al. [28] proposed a deep learning algorithm to forecast flashover in advance based on the temperature sensor data. Different machine-learning algorithms [29–39] have been proposed to train databases and pre-establish the complex relationship between sensor data and fire, so the real-time fire forecast can be achieved. Nevertheless, existing data-driven methods highly depend on the sensor data and IoT

networks inside buildings that are rarely available today or can be destroyed in fire [27,40].

Fig. 1. Smoke and fire behaviors outside the building from different views [41–43].

Comparatively, the fire and smoke images outside the room and building are more direct information that can be easily observed by people and cameras (Fig. 1). For compartment fires, the smoke is an early signal for the fire occurrence that can leak outside in the ignition and growth stages. When the fire becomes fully developed, the external smoke also has many unique behaviors and characteristics, such as the smoke velocity and color, spilled flame, and oscillation frequency. In-depth analysis of external smoke images via deep learning methods can deliver valuable information about the state and development of compartment fires.

This work explores the feasibility of using simulated external smoke images to predict the transient HRR inside the building in real-time. The fire inside a room with different growth rates, opening sizes, and fuel types are simulated to form a big database. The external smoke images rendered by CFD software are labeled with HRRs to train the deep-learning model. Finally, the proposed smoke-image-based fire forecast system is demonstrated by arbitrary dependent fire scenarios.

2. Methods

The fire HRR (or the fire size/power) is the key parameter to reflect the building fire scenarios, and it changes with time because of the fire spread and the burning of different fuels. The value of real-time HRR cannot be directly measured in real fire incidences to support firefighting operations. Nevertheless, there is a strong correlation between the fire size and the smoke generated. Although the internal fire and smoke are invisible in real fires, the visible external smoke can be easily observed and recorded to train the AI algorithm and predict the total fire HRR.

To train the deep learning algorithm, a large number of external smoke images are needed. As the first demonstration, external smoke images generated by the CFD fire simulations are used to form a relatively clean database. Compared with the photos and videos of smokes taken from fire tests, the numerical images are independent of background light, camera settings, and experimental interferences. Thus, they are applied to demonstrate the smoke-image-based prediction of fire HRR.

2.1 CFD fire model and database formation

Similar to the previous research [18,36,44], the CFD model is established firstly to generate a big database of compartment fires. In this study, a full-scale ISO 9705 compartment [45] is chosen. and established in FDS 6.7.5 [46] to simulate different fire scenarios. The default Large Eddy Simulation (LES) with a single-step and mixing-controlled combustion model is adopted to solve the smoke and heat transport from fires and the soot is modeled as $C_{0.9}H_{0.1}$ to show the smoke behavior. As shown in Fig. 2a, the compartment model consists of a 3.6 m (*length*) by 2.4 m (*width*) by 2.4 m (*height*) room and a 2.4 m (*length*) by 2.4 m (*width*) by 4.8 m (*height*) open area. The window is set at the center of the wall between the room and the open area to allow the transportation of fresh air and smoke. The open area extended outside the building resolves the flow field outside and captures the external smoke characteristics. The thermal properties of building walls and other components specified in the CFD model are recommended by NIST [47,48] that has been validated by many full-scale experiments [49] and showed that the CFD model can simulate full-scale compartment fires well.

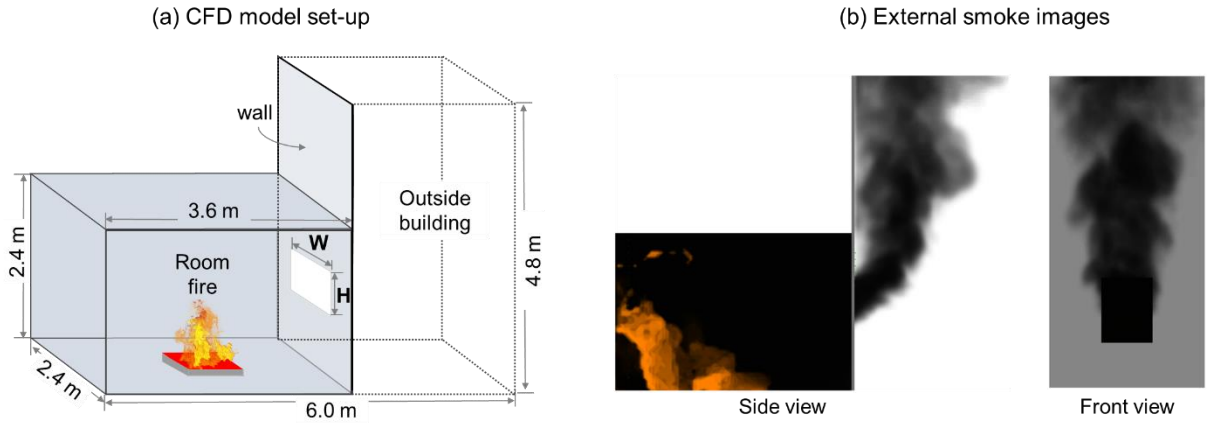

Fig. 2. Illustration of (a) the CFD model for a room and the outside open area, and (b) numerically generated smoke images.

A large number of numerical fire tests are designed to obtain one-to-one correspondences between HRRs and external smoke images (side and front views in Fig. 2b) under different fire scenarios. Three key parameters are varied in these simulations, including the fire HRR, window size, and soot yield.

(1) **HRR**. For the training database, the constant HRR is used by applying a constant fuel mass flux. The maximum HRR is set as $1500AH^{1/2}$ kW [50,51] for each opening condition. Above this critical HRR, the fire inside transforms from fuel control to ventilation control, and the spilled flame is observed. In total, 41 values of HRR from 0 to $1500AH^{1/2}$ kW are selected, and selected HRRs are evenly distributed within the range.

(2) **Window size**. The window serves as the main and only opening for the smoke outlet, and its size controls the ventilation factor ($AH^{1/2}$) and the maximum fire HRR. Nine different window sizes are selected based on the common designs, where its widths and heights are from 0.6 m to 1.0 m.

(3) **Soot yield**. The soot yield affects the intensity and color of the smoke plume outside the building. Even under the same HRR, burning different materials will produce different spilled smoke plumes. Considered all the fuel inside the building is composed of natural material (i.e., wood) and synthetic materials (i.e., polyurethane) [24], the soot yield rate (SYR) is set from 0.015 kg/kg to 0.1 kg/kg [52].

Table 1 provides a summary of these parameters in the fire models. In total, 1,845 building fire scenarios are simulated to build the fire database. According to the different sizes of windows, the selected HRR in the room ranges from 10 kW to 1500 kW, representing the peak HRR from a wastebasket to a mattress fire [53]. It is worth noting that the HRR in the model is set by the mass flow rate of gases fuel, which is not necessarily burnt instantaneously inside the room. The simulation time was set as 600 s for each fire scenario, which is sufficient to display the filling process of the fire smoke and a quasi-steady-state process with a relatively stable HRR.

Table 1. Parameters of compartment and fire in the CFD model.

Parameter	Range	Number
HRR (kW)	$0-1500AH^{1/2}$	41
Soot yield (kg/kg)	0.015, 0.04, 0.06, 0.08, 0.1	5
Window width (m)	0.6, 0.8, 1.0	3
Window height (m)	0.6, 0.8, 1.0	3
Total		1845

For all simulations, the fire source is placed at the center of the room. During the fire process, the smoke fills the entire room and overflows through the window, which can be the most easily accessible indicator for determining the fire HRR. For fast identification of internal fire scenarios, the external smoke images, both the side view (Fig. 2-b) and the front view (Fig. 2-c), are used as the indicators for determining the time-dependent fire HRR. All smoke images from front and side views rendered by Smokeview [54] are extracted to form a large database.

The grid size not only determines the accuracy of the simulation results [55,56] but also affects the quality of the exported smoke images. A grid sensitivity analysis was conducted for a base case, where the compartment fire has an opening of 0.8 m × 1.0 m, an HRR of 600 kW, and a soot yield rate of 0.1 kg/kg. Four different grid resolutions were considered, including 0.2 m, 0.1 m, 0.05 m, and 0.04 m. In all simulations, a semi-steady condition is reached in a few minutes and the average temperature and horizontal velocity from 400 s to 600 s (semi-steady condition) at the middle of the opening plane are shown in Fig. 3. Based on the grid sensitivity analysis, the temperature and horizontal velocity distribution at the middle of the opening plane, as well as the image grayscale (see Fig. A1), no longer change when using the grid size of 0.05 m or smaller. Thus, the grid size of 0.05 m is sufficient to guarantee the grid independence of the computational results.

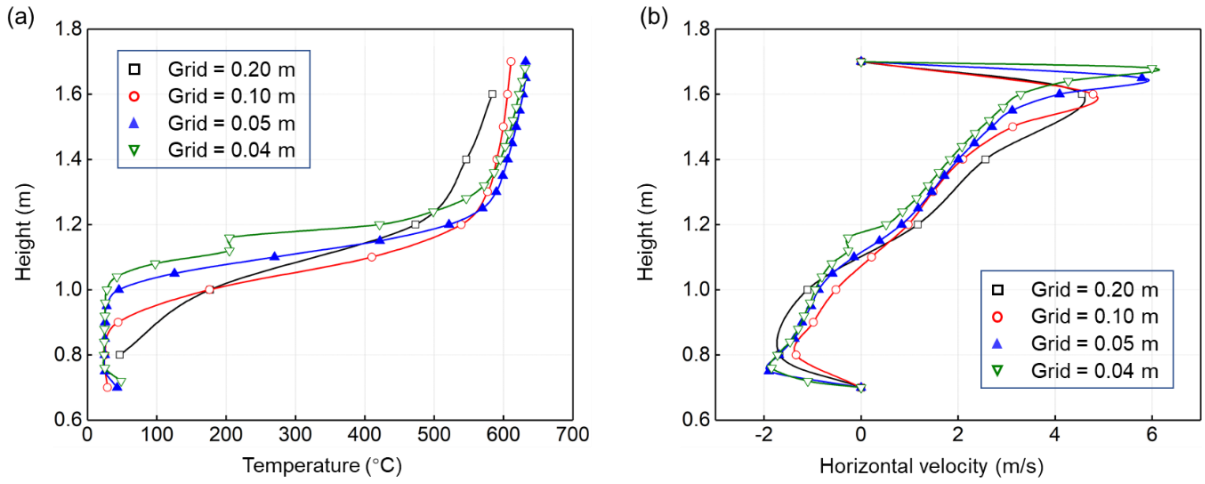

Fig. 3 Grid resolution effect on the distribution of (a) temperature and (b) horizontal velocity at the middle of the opening (0.8 m × 1.0 m), where the fire HRR is 600 kW.

2.2 External smoke images and behaviors

In this work, the smoke images rendered by the software of Smokeview are used for training the deep learning model. Before training, we should first confirm whether the rendered smoke images have different features at different HRRs and different soot yields (or fuel types). The tested fire scenario consists of ISO 9705 compartment with an opening of 0.8 m × 1.0 m under different fire HRRs and fuel soot yield rates. Fig. 4a shows the smoke images rendered by Smokeview are randomly selected, and with the same fuel and soot yield rates, the smoke becomes denser as the HRR increases (see Video S1).

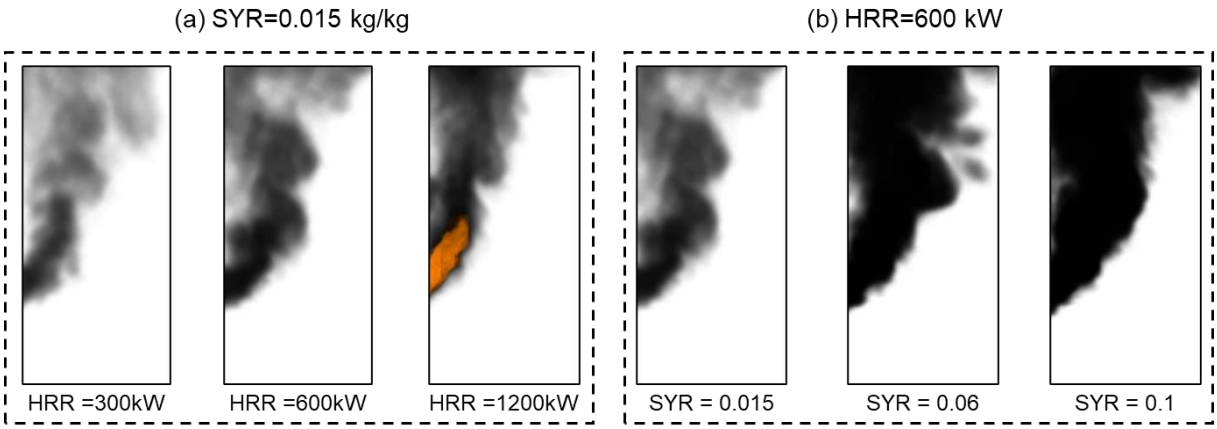

Fig. 4. Rendered smoke images (side view) (a) under different HRRs while the same soot yield rate (SYR) of 0.015 kg/kg, and (b) with different SYRs while the same fire HRR of 600 kW (see Video S1).

When the fire HRR rises and approaches the critical value of a ventilation-control fire, the spilled flame and smoke appear at the same time. These rendered smoke images with different features can be used as a basis for HRR prediction. Fig. 4b show that under the same fire HRR, burning different fuels with different soot yield rates shows very different smoke color and dynamic behaviors (also see Video S1). Burning a sooty fuel can produce denser and darker smoke, so that smoke images rendered by

software can represent the real smoke characteristics, despite certain simplifications. During the training stage of the AI model, external smoke images in over-ventilated and under ventilated stage as well as with different fuel type were considered. If the AI model can predict the pre-set fire HRR based on the rendered smoke image, it has a great potential for using real external smoke images to identify fire inside the building.

2.3 Dataset pre-processing

As the external smoke behavior is a dynamic process, and even if the same HRR is set, the actual HRR and smoke behavior can be different due to the smoke flow oscillation or the breathing effect [57] of the compartment fire, 50 frames of smoke images from a quasi-steady fire process are randomly selected in each fire scenario, whose purpose is to collect as many different characteristics of smoke as possible at the same heat release rate. Finally, a database with a total of 184,500 smoke images is formed, where each fire scenario is described by using 50 front-view images and 50 side-view images. Each smoke image in the database corresponds one-to-one with the transient HRR.

After the image database was prepared, the data pre-processing (Fig. 5) is required to make the data better adapt for training the AI model to identify the fire information. First, image clips are needed to keep only the smoke image near the window. When the smoke fills the room, the excess smoke spills out of the building through the opening. The characteristics of the smoke near the window strongly depend on the HRR inside the building. Comparatively, the smoke farther away from the window is free to diffuse, which is controlled by the external flow, rather than in-building fires. Therefore, a region of about 1.1 m × 1.1 m from the front view and side view of the external smoke image, including the upper half of the opening, is selected as the target area for the training of the deep learning model.

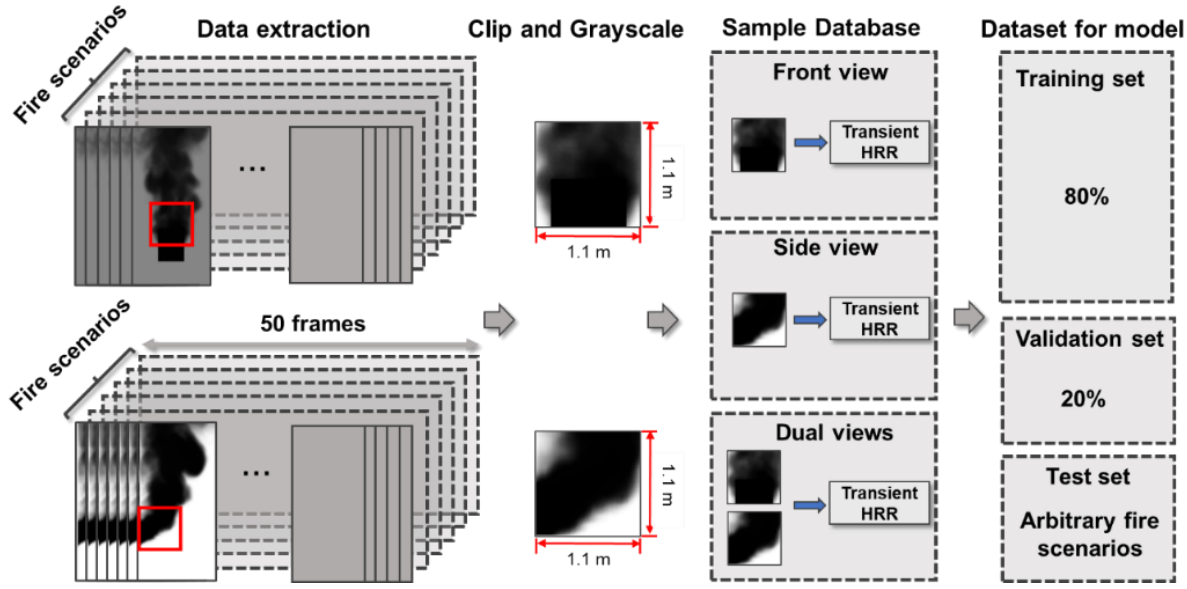

Fig. 5. Dataset pre-processing and classification for training, validation, and test.

Afterward, the clipped RGB image needs to go through a grey scaling process to reduce the data volume and effects of the background. The converted grayscale image still provides a good representation of the smoke characteristics, including the concentration and behavior of the smoke. Finally, all these images and their corresponding HRRs form the training set for the AI model. These data are further divided into two parts, the training set (80%) for training the model and the validation set (20%) for evaluating the performance of the model while training. The same process was also carried out for arbitrary fire scenarios to test the performance of the model after training. Because both front and side views of the external smoke are acquired, there are three different inputs of the AI model, i.e., only the front view, only the side view, and both views of the smoke. The performance of models trained using different views of the external smoke is discussed in Section 3.

2.4 Deep learning algorithm

Although the external smoke image can reflect the change of HRRs, it is hard for our eyes to recognize different external smoke behaviors. Thus, convolutional neural network (CNN) is introduced to process these images and differentiate one from the other. Compared with primitive image processing algorithms that require manual feature extraction, CNN has the ability to capture the spatial and temporal dependencies in an image automatically after enough training. VGG [58] is a very classical CNN architecture for image classification, which was proposed in 2014 by the Visual Geometry Group. While it has been widely used in object detection [59], face recognition [60], and traffic sign recognition [61], it is the first time that VGG is applied to evaluate the fire size in building fire quantitatively. The performance of the VGG architecture of predicting fire inside the building based on external smoke images is explored. In this paper, VGG16 is used to extract characteristics of smoke under different building fire scenarios and obtain the relationship between smoke characteristics and HRRs.

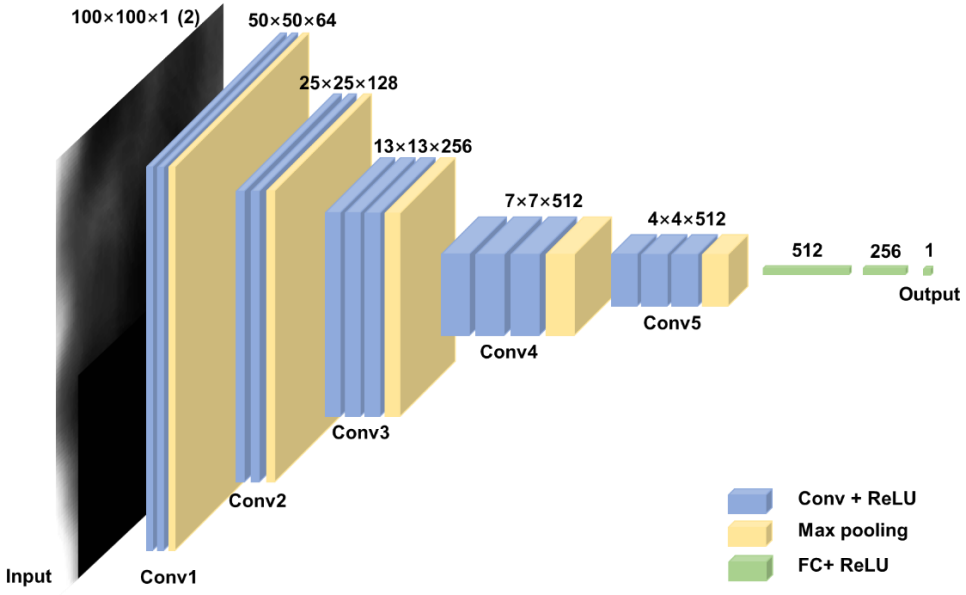

Fig. 6. The architecture of VGG16 in AI-driven fire prediction based on external smoke images.

The detailed architecture of VGG16 is depicted in Fig.6, consisting of 13 convolutional layers, five max pooling layers, and three fully-connected layers. Several consecutive 3×3 convolutional kernels are adopted in VGG instead of the larger convolutional kernels in previous work [62,63]. The continuous use of these small convolutional kernels can reduce the parameters of the convolutional kernel and increase the network depth to enhance the learning ability of the CNN for image features. The feature maps generated by the convolutional operation are passed layer by layer, and the max-pooling layer after the convolutional layer is responsible for reducing the dimension of the feature map and extract dominant features. Finally, the original smoke image with the dimension of 100×100×1 (front view and side view) or 100×100×2 (dual views) is reduced to 4× 4 × 512. These feature maps are flattened into a column vector to establish the non-linear relationship with the final output through the fully connected layer.

The entire network structure contains a total of 19 million parameters, which is sufficient to extract minute features of each smoke image. ReLU is selected as the activation function in all convolutional layers and fully connected layers, and the loss function MSE is used to compare the difference between actual and predicted values. Dropout is applied after each max pooling layer and fully connected layer with a dropout rate of 0.3 to avoid overfitting. A server with 32 CPU cores and a Tesla P100 GPU card is adopted to run the model, and it takes about 4 h in total for 100-step training.

3. Results and discussion

The AI-driven prediction of fire HRR based on external smoke images was demonstrated in both constant HRR and transient HRR cases in this section. First, the AI model was trained by using all fire scenarios with a constant HRR, and then, its performance was judged by the validation set with constant HRR. In the model training process, the external smoke images extracted from fires with constant HRR were used to train the AI model. Two different fire scenarios were predicted, (1) the fuel type and soot yield are known and (2) neither the fuel type nor soot yield is known.

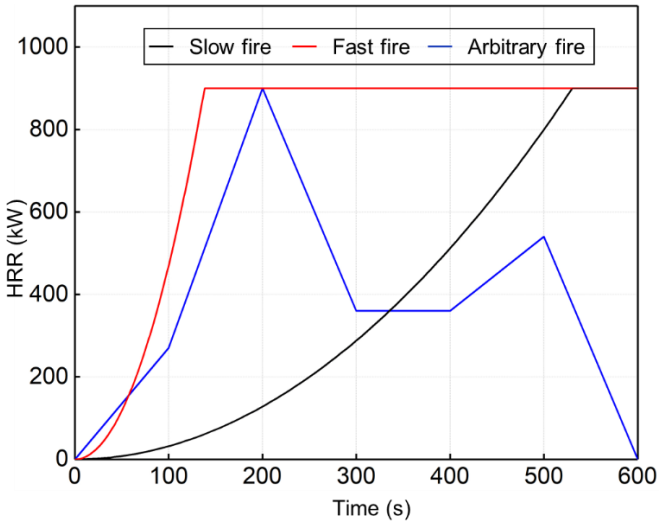

Fig. 7. Three specified HRR ramps (slow, fast, and arbitrary) for testing the AI prediction of transient fires.

Afterward, the AI model was further tested by the time-dependent HRR in an actual fire. Three different prespecified HRR ramps were set with a peak HRR of 900 kW, as shown in Fig.7. Specifically, two standard t-squared fire HRR curves were tested, one with a growth factor of 0.0032 kW/s^2 (slow fire) and one with a growth factor of 0.047 kW/s^2 (fast fire) [51]. The third arbitrary ramp represents a random fire process with several HRR increasing and decreasing processes. These prespecified HRRs were set in fire scenarios with the opening size of 0.7 m (width) ×1.1 m (height) and two soot yields of 0.015 kg/kg and 0.043 kg/kg.

3.1 Validation with constant HRR

First, the fire with known fuel types is studied, where the soot yield rate of 0.015 kg/kg (wood) is considered in the model training. The AI model only needs to be trained using external smoke images from fires with a smoke yield rate of 0015 kg/kg. Fig. 8a shows losses and determination coefficients (R^2) of training and validation during the training process. After 100 steps of training, each model reaches convergence with a maximum MSE loss of 3580 and a minimum R^2 of 0.962, which indicates that all three models can well predict the fire HRR inside the building. The R^2 of the dual-view model even reached 0.97, so its prediction performance is the highest, compared to the other two models trained by the single-view smoke images.

Predicting the transient fire HRR without known the type of burning fuel is more complex. Without the information of the fuel type and the soot yield, more external smoke images from the compartment fire with different soot yield rates are needed for AI model to identify more detailed patterns of smoke plumes. Thus, external smoke images from fires with different HRR and fuel types (soot-yield rates) are used to train the AI model. After the same steps of training, losses and R^2 of training and validation in this case are shown in Fig. 8b. Although the loss of the training set decreases with iteration, the validation loss becomes stable in advance and cannot reach the same value as the training set, which is caused by the compensation effect between the fuel soot yield rate and fire HRR, for example, a small fire on a fuel of a large soot yield can produce a smoke plume that is similar to a large fire on a fuel of a small soot yield.

The smoke images rendered by Smokeview are only related to the soot densities computed by FDS. However, both the increase of HRRs and SYRs can lead to an increase in soot density. As a result, fire scenarios with different SYRs and HRRs may produce similar external smoke images, leading to misjudgment of AI models trained by rendered smoke images. This situation can be significantly improved if the model is trained by real smoke images, as more color features exist in real smoke images from actual fires. Nevertheless, the coefficient of determination for all three models can achieve a minimum value of 0.890, which shows that the external smoke image still reflects the HRR of a room fire with unknown fuel types. Meanwhile, the dual-view model has excellent performance during the training with an R^2 of 0.923.

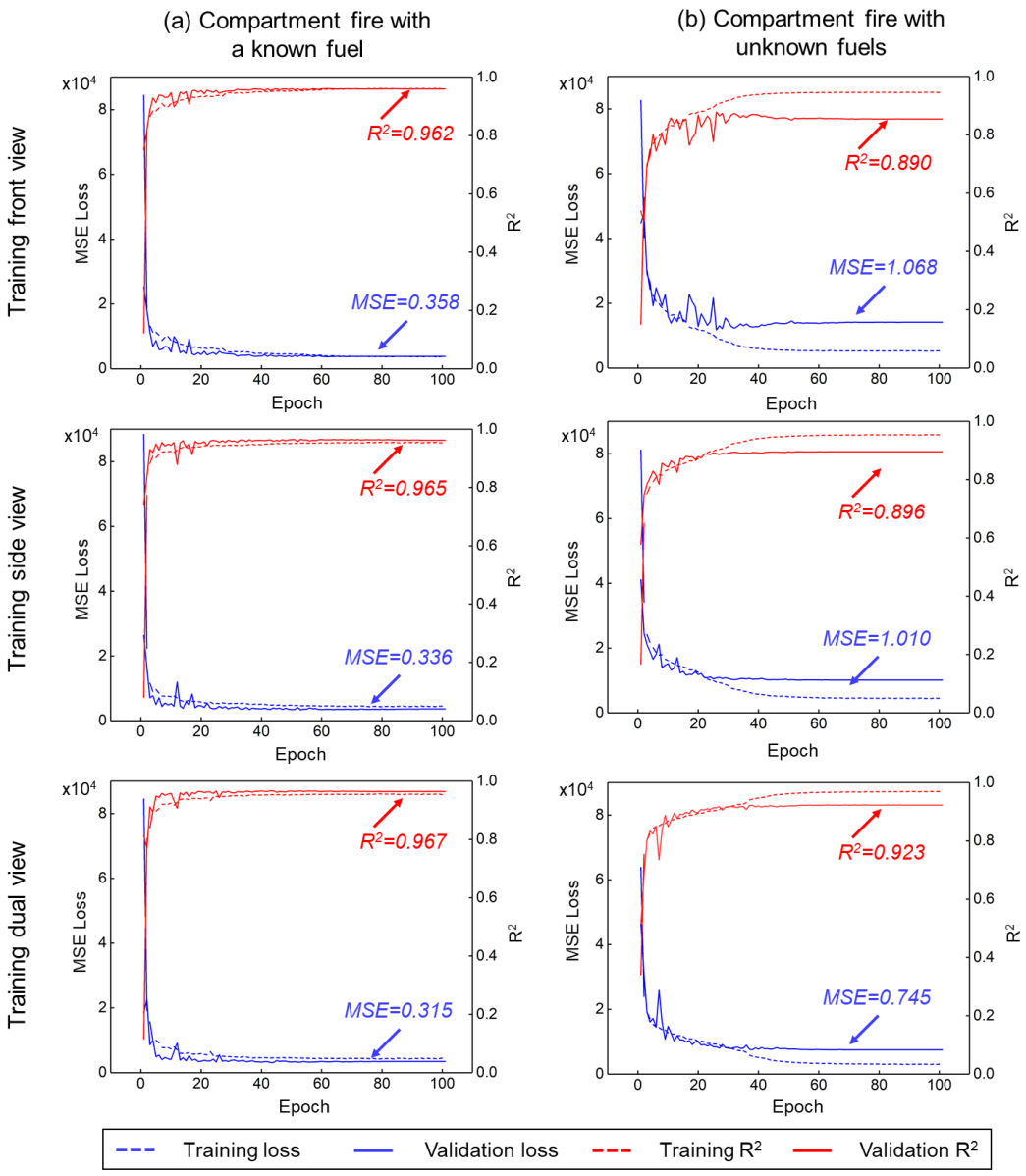

Fig. 8. Losses and R^2 of training and validation during the training process: (a) fire with a known fuel type; (b) fire with unknown fuel types.

3.2 Predicting the transient HRR of fire with a known fuel

Any real building fire will be transient and complex, and its HRR changes with time. To apply the deep learning model in a real building fire, identifying the time-dependent HRR by the external image is needed. Herein, with an opening of 0.7 m (*width*) ×1.1 m (*height*) and a known fuel type (wood, soot yield rate of 0.015 kg/kg), three different HRR ramps representing slow fire growth, fast fire growth, and arbitrary fire evolution in Fig.7 are predicted using the AI models trained by smoke images from different angles.

The arbitrary fire evolution predicted by the dual-view model is taken as an example to show the real-time performance of the AI model. The detailed prediction process for the transient fire HRR using

the front view and side view of the external smoke image is demonstrated in Video S2. In general, the prediction of AI showed high accuracy throughout the fire development process. Fig. 9 compares the predicted fire HRRs at different stages of fire development, which shows that the evolution of AI's prediction is well consistent with a real fire.

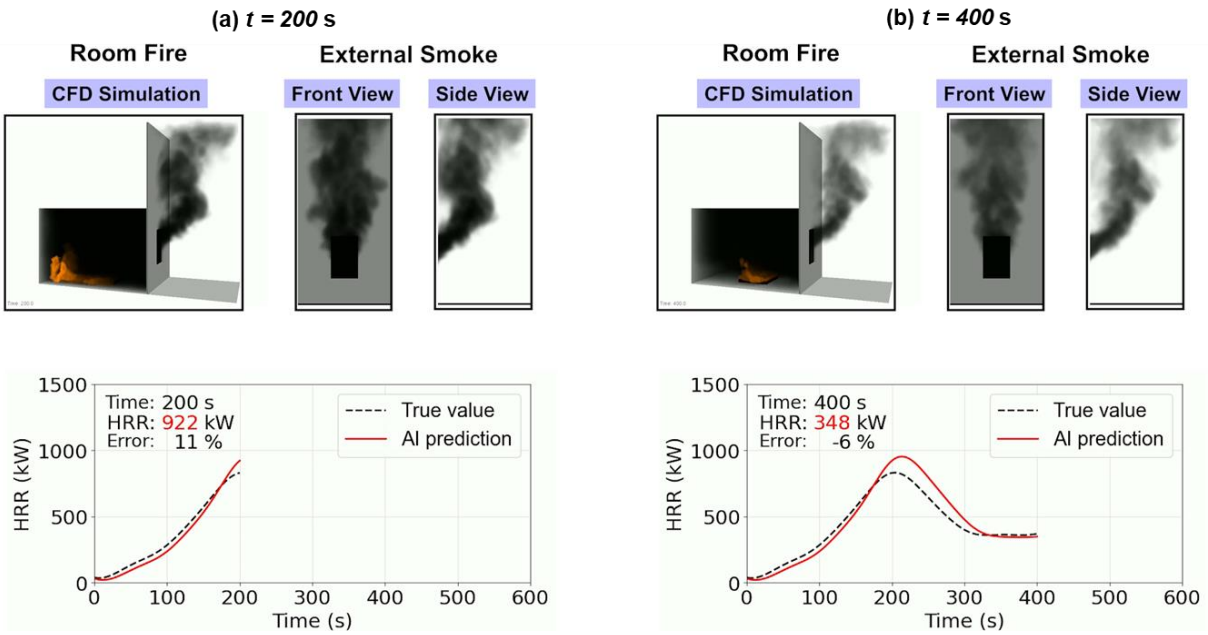

Fig. 9. Real-time HRR prediction process using dual view external smoke images from a fire that burns a known fuel with a constant soot yield rate, (a) t = 200 s, and (b) t = 400 s (see Video S2).

Fig. 10 summarizes the comparison between the true HRR and the predicted HRR. An FFT filter is used to reduce the impact of noise. Overall, all three models can achieve accurately determine the time-dependent fire HRRs, and among three, training the front view model shows the best performance. Although the side view and dual-view model tend to overestimate the real-time HRR, the overall error of all three approaches is no more than 20%. On the other hand, a moderate overestimation can provide some safety margin for firefighting activities and decision making.

For the slow fire, since the low fire growth factor allows for adequate smoke development, the HRR growth can be well predicted by these AI models with a relative error of ±10%, as shown in Fig. 10a. For the fast fire, rapid HRR growth often causes a delay in the AI prediction, but the error is still no more than 20%. Although both the side-view and dual-view models over-estimate the fire HRR, their prediction gradually approaches the actual value of HRR as the fire develops. For the 3rd arbitrary fire case, including several HRR growth and decay processes, the error of AI models is still within 20% in Fig.10c. When the fire HRR changes rapidly, the predicted HRR has some delay, which is caused by the delay in smoke propagation. In other words, the AI model underestimates the actual HRR when the HRR increases rapidly and overestimates it when the fire decays rapidly.

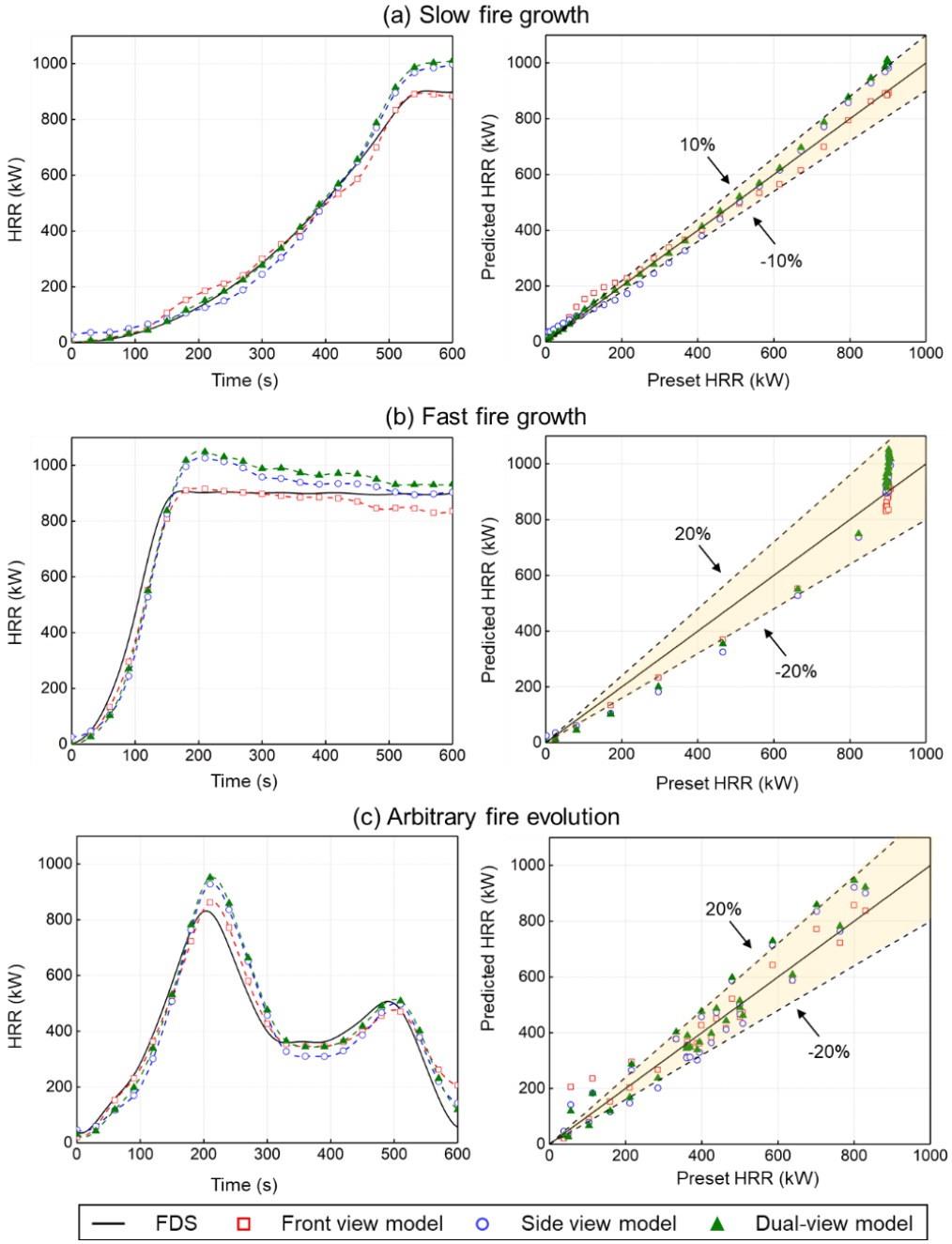

Fig. 10. Comparisons of the pre-set transient HRR in the CFD fire simulations and the AI prediction, (a) slow fire growth; (b) fast fire growth; (c) arbitrary fire evolution.

In summary, all these results show that the proposed AI model can well capture the characteristics of external smoke images and predict transient fire HRR inside the building. The superior performance of VGG16 suggests that it could be used as a basic framework for identifying and predicting the hidden building fire scenarios. In terms of performance, using both front and side views of smoke can give a safer prediction because it always slightly overestimates the HRR. However, it also needs smoke images taken from two different angles, which may not be available in real fire scenes. If the smoke image from only one camera from either front or side view is available, the fire HRR can still be identified accurately with an error < 20%.

3.3 Predicting the transient HRR with unknown fuels

In a real fire event, it is often difficult for firefighters to know what is burning inside the building. Various combustible items make the fire and burning process more complex, and different fuels will produce different smoke yields when they burn together. Therefore, to achieve accurate HRR prediction based on external smoke images, the AI model needs to adapt to fire scenarios with different smoke yields. Thus, external smoke images of fires with different soot yield rates from natural material and synthetic materials are used to train the AI model, and fires with SYR of 0.043 kg/kg are used to test the generalized performance of the AI model.

The prediction of the arbitrary fire evolution was demonstrated at different moments in Fig. 11 by using the dual-view smoke images as an example. The detailed comparison of fire HRR evolution can be seen in Videos S3. Results showed that even for fires with unknown fuel types, using external smoke images could well identify the fire development hidden inside the building.

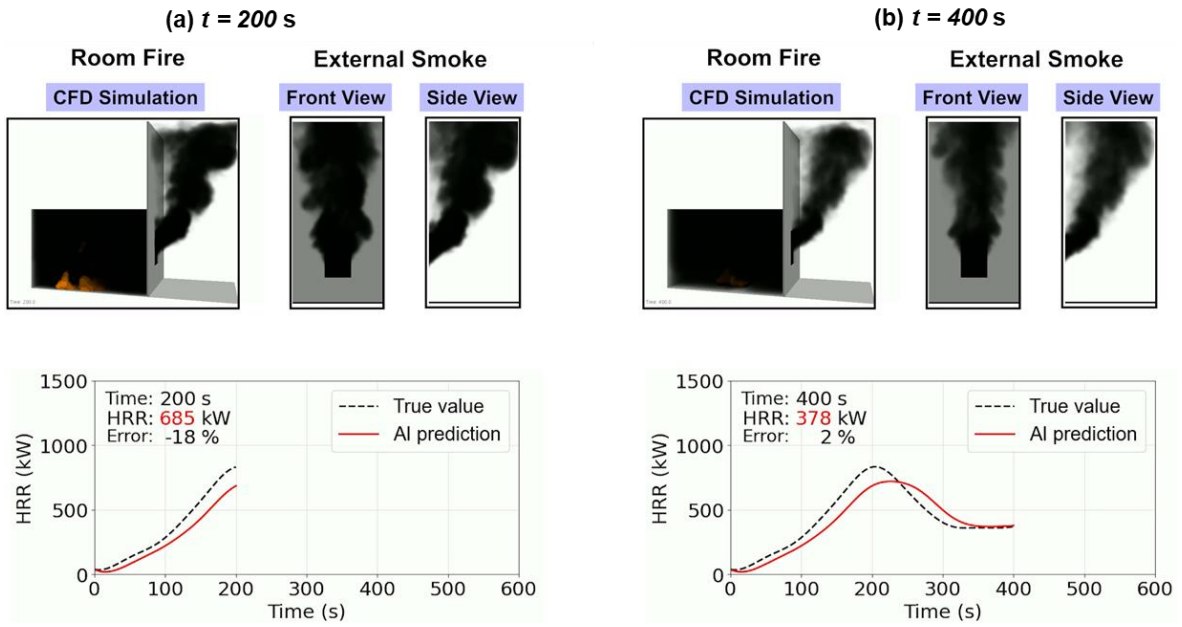

Fig. 11. Real-time HRR prediction process by AI under transient fire with the unknown fuel and soot yield rate, (a) t = 200 s, and (b) t = 400 s (see Video S3).

The detailed performance of each model for different fire scenarios are shown in Fig.12. The results demonstrated that the AI models still can well determine the fire development without knowing specific fuel types. Although external smoke images become more complex from a fire with unknown fuel types, the proposed model still shows acceptable predictions, with a relative error of less than 20% except for the fast fire scenario. For the fast fire scenario, the error is mainly caused by the delayed propagation of the smoke. Although the fire HRR increases a lot in a short period of time, it still takes some time for the smoke to escape from the openings. This will lead to an overall underestimation of the HRR and can be mitigated when the fire develops smoothly, as shown in Fig.12b.

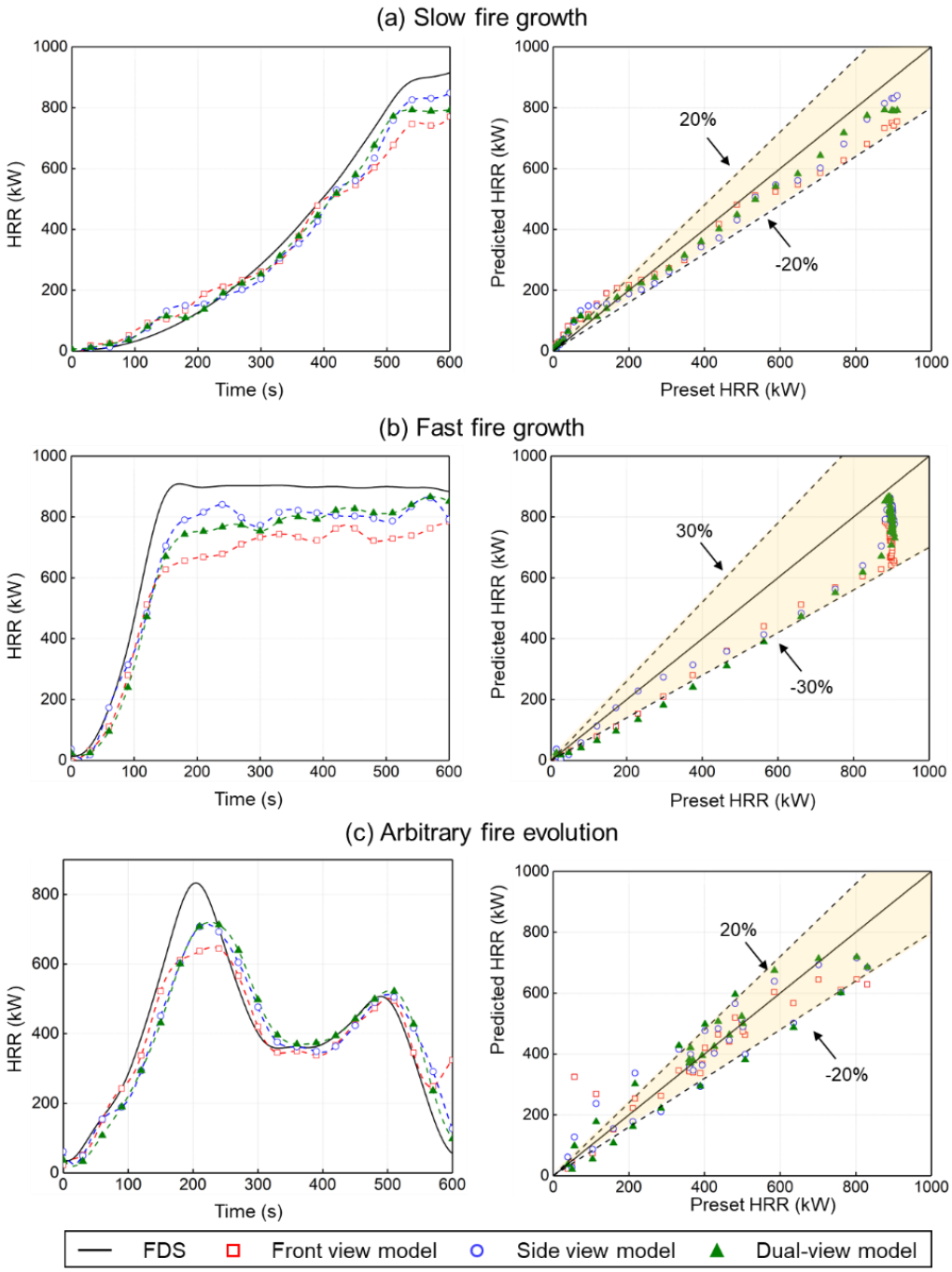

Fig. 12. Comparisons of the model predictions to the FDS simulations: (a) slow fire growth; (b) fast fire growth; (c) arbitrary fire evolution.

Comparing the performance of the three models in slow fire growth, fast fire growth, and arbitrary fire evolution scenarios, the dual view model always gives a relatively accurate prediction of fire HRR even in the decay stage of the compartment fire. This suggests that the increase of smoke images provided to the model is beneficial in improving the performance of the AI model to some extent. Besides, the front view model and side view model can achieve prediction accuracy comparable to that of the dual-view model with a relative error of 20%. These two models show large prediction errors in the low fire HRR stage, which are caused by the early-stage smoke filling and continuous smoke

spillage in the decay phase (see Fig.12c). However, the early fire stage and decay stage with a low HRR is not so important in firefighting operation, compared to the increasing stage with a high HRR, so the model trained by the front-view or side-view smoke images is also a competitive option. Thus, AI's identification of the fire HRR inside the building based on external smoke images is also effective and accurate, if the external fire smoke is only taken by one camera and from one angle.

4. Conclusions

In this work, the prediction for building fire HRRs using smoke images outside the building and deep learning method is presented and demonstrated for the first time. A series of ISO 9705 compartment fire cases are simulated by CFD code to form a fire database, and smoke images rendered by Smokeview are used to train the prediction model. VGG16 is demonstrated as an effective way to extract features from smoke images and achieve accurate HRR prediction, and it provides an effective framework for the prediction of building fire HRR and other information.

Results show that when the fuel inside the building is known, the AI's prediction of fire HRR is extremely accurately ($R^2 > 0.962$) by using either single or dual smoke images. If the burning fuels are unknown, AI can still give a reasonable prediction of the fire HRR inside the building ($R^2 > 0.89$). We also found that using dual-view smoke images can predict a more accurate fire HRR. Nevertheless, even if the smoke images are taken from only one angle, either the front view or the side view, the AI model can still predict the transient fire HRRs with an error of no more than 20%.

The present work is validated by a relatively clean database of synthetic smoke images, which is independent of background light, camera settings, and experimental interferences. However, the situation in real fire scenarios could be very complicated. Thus, the numerical demonstration of the AI method is only the first step. In the future, we will continue to test the performance of the AI model through real experiments, in which the ventilation condition such as the number of openings, the layout of the building, and the background are complex. Overall, this work paves the way for using actual external smoke images to predict fire information inside the building, which will facilitate the development and application of AI-driven smart firefighting systems.

Acknowledgments

This work is funded by the Hong Kong Research Grants Council Theme-based Research Scheme (T22-505/19-N), National Natural Science Foundation of China (NSFC grant no. 52108480), and the PolyU Emerging Frontier Area (EFA) Scheme of RISUD (P0013879). TZ thanks the support from the Hong Kong PhD Fellowship Scheme.

Declaration of Competing Interest

The authors declare that they have no known competing financial interests or personal relationships that could have appeared to influence the work reported in this paper.

References

[1] Babrauskas V, Peacock DR. Heat release rate: the single most important parameter in fire hazard. Fire Saf J 1992;18:255–72.

[2] Karlsson B, Quintiere J. Enclosure Fire Dynamics. 1999. https://doi.org/10.1201/9781420050219.

[3] McCaffrey BJ, Quintiere JG, Harkleroad MF. Estimating room temperatures and the likelihood of flashover using fire test data correlations. Fire Technol 1981;17:98–119. https://doi.org/10.1007/BF02479583.

[4] Johansson N, Svensson S. Review of the Use of Fire Dynamics Theory in Fire Service Activities. Fire Technol 2019;55:81–103. https://doi.org/10.1007/s10694-018-0774-3.

[5] Koo SH, Fraser-Mitchell J, Welch S. Sensor-steered fire simulation. Fire Saf J 2010;45:193–205. https://doi.org/10.1016/j.firesaf.2010.02.003.

[6] Han L, Potter S, Beckett G, Pringle G, Welch S, Koo SH, et al. FireGrid: An e-infrastructure for next-generation emergency response support. J Parallel Distrib Comput 2010;70:1128–41. https://doi.org/10.1016/j.jpdc.2010.06.005.

[7] Choe S-H. 2 Die as Asiana Cargo Plane Crashes Off South Korea. New York Times 2011.

[8] Jahn W, Rein G, Torero JL. A posteriori modelling of the growth phase of Dalmarnock Fire Test One. Build Environ 2011;46:1065–73. https://doi.org/10.1016/j.buildenv.2010.11.001.

[9] Jahn W. Using suppression and detection devices to steer CFD fire forecast simulations. Fire Saf J 2017;91:284–90. https://doi.org/10.1016/j.firesaf.2017.03.062.

[10] Sundström B, Wickström U. Fire: Full Scale Tests 1981.

[11] AI A, Holmlund C, MA K. Effects of ignition source in room fire tests. Fire Sci Technol 1987;7:1_1-1_13.

[12] Kurzawski AJ, Ezekoye OA. Inversion for fire heat-release rate using heat flux measurements. J Heat Transfer 2020;142:1–11. https://doi.org/10.1115/1.4046264.

[13] Richards RF, Munk BN, Plumb OA. {Fire Detection, Location and Heat Release Rate Trough Inverse Problem Solution. Part II: Experiment}. Fire Saf J 1997;28:323–50. https://doi.org/10.1016/S0379-7112(97)00005-2.

[14] Richards RF, Ribail RT, Bakkom AW, Plumb OA. Fire detection, location and heat release rate through inverse problem solution. Part II: Experiment. Fire Saf J 1997;28:351–78. https://doi.org/10.1016/S0379-7112(97)00006-4.

[15] Price M, Marshall A, Trouvé A. A Multi-observable Approach to Address the Ill-Posed Nature of Inverse Fire Modeling Problems. Fire Technol 2016;52:1779–97. https://doi.org/10.1007/s10694-015-0541-7.

[16] Jahn W. Inverse Modelling to Forecast Enclosure Fire Dynamics 2010.

[17] Jahn W, Rein G, Torero JL. Forecasting fire growth using an inverse zone modelling approach. Fire Saf J 2011;46:81–8. https://doi.org/10.1016/j.firesaf.2010.10.001.

[18] Jahn W, Rein G, Torero JL. Forecasting fire dynamics using inverse computational fluid dynamics and tangent linearisation. Adv Eng Softw 2012;47:114–26. https://doi.org/10.1016/j.advengsoft.2011.12.005.

[19] Overholt KJ, Ezekoye OA. Characterizing Heat Release Rates Using an Inverse Fire Modeling Technique. Fire Technol 2012;48:893–909. https://doi.org/10.1007/s10694-011-0250-9.

[20] Kim JH, Lattimer BY. Real-time probabilistic classification of fire and smoke using thermal imagery for intelligent firefighting robot. Fire Saf J 2015;72:40–9. https://doi.org/10.1016/j.firesaf.2015.02.007.

[21] Wu X, Park Y, Li A, Huang X, Xiao F, Usmani A. Smart Detection of Fire Source in Tunnel Based on the Numerical Database and Artificial Intelligence. Fire Technol 2021;57:657–82. https://doi.org/10.1007/s10694-020-00985-z.

[22] Wu X, Zhang X, Huang X, Xiao F, Usmani A. A real-time forecast of tunnel fire based on numerical database and artificial intelligence. Build Simul 2021. https://doi.org/10.1007/s12273-021-0775-x.

[23] Wu X, Zhang X, Jiang Y, Huang X, Huang GGQ, Usmani A. An intelligent tunnel firefighting system and small-scale demonstration. Tunn Undergr Sp Technol 2022:104301. https://doi.org/10.1016/j.tust.2021.104301.

[24] Su L chu, Wu X, Zhang X, Huang X. Smart performance-based design for building fire safety: Prediction of smoke motion via AI. J Build Eng 2021;43:102529. https://doi.org/10.1016/j.jobe.2021.102529.

[25] Zeng Y, Zeng Y, Zhang X, Su L, Wu X, Huang X. An AI-Driven Intelligent Tool for Building Fire Safety Analysis and Performance-Based Design. J Build Eng (under Rev 2021.

[26] Dexters A, Leisted RR, Van Coile R, Welch S, Jomaas G. Testing for knowledge: Application of machine learning techniques for prediction of flashover in a 1/5 scale ISO 13784-1 enclosure. Fire Mater 2020:1–12. https://doi.org/10.1002/fam.2876.

[27] Wang J, Tam CW, Jia Y, Peacock R, Reneke P, Yujun E, et al. P-Flash – A machine learning-based model for flashover prediction using recovered temperature data. Fire Saf J 2021;122:103341. https://doi.org/10.1016/j.firesaf.2021.103341.

[28] Huang X, Hom H, Zhang T, Zhang T, Wang Z, Wong HY, et al. Real-time Forecast of Compartment Fire and Flashover based on Deep Learning. Fire Saf J (under Rev 2021.

[29] Lee EWM, Yuen RKK, Lo SM, Lam KC, Yeoh GH. A novel artificial neural network fire model for prediction of thermal interface location in single compartment fire. Fire Saf J 2004;39:67–87. https://doi.org/10.1016/S0379-7112(03)00092-4.

[30] Yuen RKK, Lee EWM, Lo SM, Yeoh GH. Prediction of temperature and velocity profiles in a single compartment fire by an improved neural network analysis. Fire Saf J 2006;41:478–85. https://doi.org/10.1016/j.firesaf.2006.03.003.

[31] Huang Y, Chen X, Xu L, Li K. Single Image Desmoking via Attentive Generative Adversarial Network for Smoke Detection Process. Fire Technol 2021;57:3021–40. https://doi.org/10.1007/s10694-021-01096-z.

[32] Guo S, Yang R, Zhang H, Zhang X. New inverse model for detecting fire-source location and intensity. J Thermophys Heat Transf 2010. https://doi.org/10.2514/1.46513.

[33] Overholt KJ, Ezekoye OA. Quantitative Testing of Fire Scenario Hypotheses: A Bayesian Inference Approach. FIRE-D-14-00163 Ref[16] Fire Technol 2015;51:335–67.

https://doi.org/10.1007/s10694-013-0384-z.

[34] Chu YY, Kodur VKR, Liang D. A Probabilistic Inferential Algorithm to Determine Fire Source Location Based on Inversion of Multidimensional Fire Parameters. Fire Technol 2017;53:1077–100. https://doi.org/10.1007/s10694-016-0620-4.

[35] Kurzawski A, Cabrera JM, Ezekoye OA. Model Considerations for Fire Scene Reconstruction Using a Bayesian Framework. Fire Technol 2020;56:445–67. https://doi.org/10.1007/s10694-019-00886-w.

[36] Buffington T, Cabrera JM, Kurzawski A, Ezekoye OA. Deep-Learning Emulators of Transient Compartment Fire Simulations for Inverse Problems and Room-Scale Calorimetry. Fire Technol 2020. https://doi.org/10.1007/s10694-020-01037-2.

[37] Cabrera JM, Ezekoye OA, Moser RD. Bayesian Inference of Fire Evolution Within a Compartment Using Heat Flux Measurements. Fire Technol 2020;57:2887–903. https://doi.org/10.1007/s10694-020-01036-3.

[38] Kou L, Wang X, Guo X, Zhu J, Zhang H. Deep learning based inverse model for building fire source location and intensity estimation. Fire Saf J 2021;121:103310. https://doi.org/10.1016/j.firesaf.2021.103310.

[39] Fang H, Lo SM, Zhang Y, Shen Y. Development of a machine-learning approach for identifying the stages of fire development in residential room fires. Fire Saf J 2021;126:103469. https://doi.org/10.1016/j.firesaf.2021.103469.

[40] Pomeroy AT. Analysis of the effects of temperature and velocity on the response time index of heat detectors 2010.

[41] John Blair. NIST Evaluates Firefighting Tactics In NYC High-Rise Test 2018. https://www.nist.gov/news-events/news/2008/03/nist-evaluates-firefighting-tactics-nyc-high-rise-test%0A.

[42] Thomson C. Vancouver firefighters douse high-rise apartment fire just in time 2021. https://www.vancouverisawesome.com/local-news/vancouver-firefighters-douse-high-rise-apartment-fire-just-in-time-photos-video-3867582.

[43] Advanced. Advanced's New EvacGo Makes Meeting the BS 8629 Code of Practice Easy 2021. https://uk.advancedco.com/news/news-repository/advanced's-new-evacgo-makes-meeting-the-bs-8629-code-of-practice-easy.aspx.

[44] Hodges JL, Lattimer BY, Luxbacher KD. Compartment fire predictions using transpose convolutional neural networks. Fire Saf J 2019;108:102854. https://doi.org/10.1016/j.firesaf.2019.102854.

[45] ISO9705, Fire Tests - Full-Scale Room Test for Surface Products First Edition. Int Organ Stand Geneva, Switz 1993.

[46] McGrattan K, Hostikka S, McDermott R, Floyd J, Weinschenk C, Overhold K. Sixth Edition Fire Dynamics Simulator User 's Guide (FDS). NIST Spec Publ 1019 2020;Sixth Edit.

[47] fds/Validation/NIST_FSE_2008 at master · firemodels/fds n.d.

[48] Lock A, Bundy M, Johnsson EL, Hamins A, Ko GH, Hwang C, et al. NIST Technical Note 1603: Experimental study of the effects of fuel type , fuel distribution , and vent size on full-scale

underventilated compartment fires in an ISO 9705 Room. 2008.

[49] McGrattan KB, Hostikka S, Floyd JE, McDermott R. Fire Dynamics Simulator, Technical Reference Guide, Volume 3: Experimental Validation. NIST Spec Publ 1018 2015;3.

[50] Lee YP, Delichatsios MA, Silcock GWH. Heat fluxes and flame heights in façades from fires in enclosures of varying geometry. Proc Combust Inst 2007;31 II:2521–8. https://doi.org/10.1016/j.proci.2006.08.033.

[51] Drysdale D. An Introduction to Fire Dynamics. 3rd ed. Chichester, UK: John Wiley & Sons, Ltd; 2011. https://doi.org/10.1002/9781119975465.

[52] Robbins AP, Wade CA. Soot Yield Values for Modelling Purposes – Residential Occupancies 2008:147.

[53] Kim HJ, Lilley DG. Heat release rates of burning items in fires. J Propuls Power 2002;18:866–70. https://doi.org/10.2514/2.6011.

[54] Forney G. Smokeview, A tool for visualizing fire dynamics simulation data - Volume 2: Technical Reference Guide, NIST SP 1017-2 2018;III.

[55] Mowrer FW, Friday PA. Comparison of FDS Model Predictions With FM/SNL Fire Test Data. 2001.

[56] McGrattan K, Floyd J, Forney G, Baum H, Hostikka S. Improved radiation and combustion routines for a large eddy simulation fire model. Fire Saf Sci 2003:827–38. https://doi.org/10.3801/IAFSS.FSS.7-827.

[57] Nuclear Energy Agency (NEA). Investigating Heat and Smoke Propagation Mechanisms in Multi-Compartment Fire Scenarios: Final Report of the PRISME Project 2018.

[58] Simonyan K, Zisserman A. Very deep convolutional networks for large-scale image recognition. 3rd Int Conf Learn Represent ICLR 2015 - Conf Track Proc 2015:1–14.

[59] Chen Z, Khemmar R, Decoux B, Atahouet A, Ertaud JY. Real time object detection, tracking, and distance and motion estimation based on deep learning: Application to smart mobility. 2019 8th Int. Conf. Emerg. Secur. Technol. EST 2019, 2019. https://doi.org/10.1109/EST.2019.8806222.

[60] Ahmadvand P, Ebrahimpour R, Ahmadvand P. How popular CNNs perform in real applications of face recognition. 24th Telecommun. Forum, TELFOR 2016, 2017. https://doi.org/10.1109/TELFOR.2016.7818876.

[61] Bi Z, Yu L, Gao H, Zhou P, Yao H. Improved VGG model-based efficient traffic sign recognition for safe driving in 5G scenarios. Int J Mach Learn Cybern 2020. https://doi.org/10.1007/s13042-020-01185-5.

[62] LeCun Y, Bottou L, Bengio Y, Haffner P. Gradient-based learning applied to document recognition. Proc IEEE 1998. https://doi.org/10.1109/5.726791.

[63] Krizhevsky A, Sutskever I, Hinton GE. ImageNet classification with deep convolutional neural networks. Commun ACM 2017. https://doi.org/10.1145/3065386.

[64] Demidenko E. Kolmogorov-smirnov test for image comparison. Lect Notes Comput Sci (Including Subser Lect Notes Artif Intell Lect Notes Bioinformatics) 2004;3046 LNCS:933–9. https://doi.org/10.1007/978-3-540-24768-5_100.

Appendix

Fig. A1 presents the grayscale histograms [64] of the external smoke image under different grid resolutions. The external smoke image from 400 s to 600 s were averaged and converted to grayscale to compare the effect of grid resolutions on the rendered smoke image. There are two peaks in the grayscale smoke image, the peak close to 0 representing the characteristics of the smoke and the other peak representing the background pixels. Based on the grid sensitivity analysis of external smoke image, the histogram of the smoke image using the grid of 0.05 m is close to the results with a finer grid. Therefore, the grid of 0.05 m is also sufficient to guarantee the grid independence of the image results.

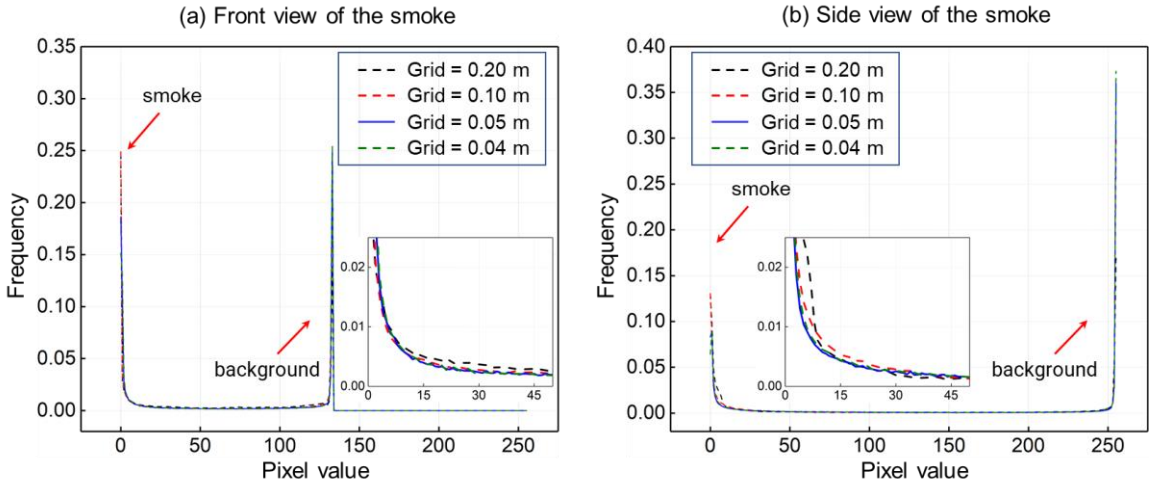

Fig. A1 Grid resolution effect on the smoke image: (a) front view of the smoke and (b) side view of the smoke.